Anomalous and linear holographic hard wall models for glueballs and the pomeron

Rafael A. Costa-Silva* and Henrique Boschi-Filho†

Instituto de Física, Universidade Federal do Rio de Janeiro, 21.941-909, Rio de Janeiro, RJ, Brazil

(Received 18 October 2023; accepted 26 March 2024; published 15 April 2024)

In this work we propose improved holographic hard wall (HW) models by the inclusion of anomalous dimensions in the dual operators that describe glueballs inspired by the AdS/CFT correspondence. The anomalous dimensions come from well known semiclassical gauge/string duality analysis showing a dependence with the logarithm of spin S of the boundary states. We show that these logarithm anomalous dimensions of the high spin operators combined with the usual HW model allow us to match the pomeron trajectory and give glueball masses that are better than that of the original HW and soft wall models in comparison with lattice data. We also build up other anomalous HW models considering that the logarithm anomalous dimensions can be approximated by a truncated series of odd powers of the difference $\sqrt{S} - 1/\sqrt{S}$. These models also fit the pomeron trajectory and produce good glueball masses. Then, we consider an anomalous dimension that is proportional to $\sqrt{S}$, providing reasonable results. Finally, we propose an asymptotic linear anomalous HW model that effective dimensions for high spins operators are of the form $\Delta = a\sqrt{S} + b$, where a and b are constants to be fixed by comparison with the soft pomeron trajectory. In this last model, the Regge trajectory is asymptotically linear even for very high spins ($J \sim 100$) matching the soft pomeron trajectory accurately and generates glueball masses with deviations with respect to the lattice data better than the original HW and soft wall models.

DOI: 10.1103/PhysRevD.109.086019

I. INTRODUCTION

QCD describes strong interactions. At high energies its coupling is small so that it can be treated perturbatively. On the other hand, at low energies, the QCD coupling is large and nonperturbative methods are needed to tackle phenomena like confinement, phase transitions, and hadronic spectra. This nonperturbative behavior usually requires involved numerical calculations known as lattice QCD. Alternatively, low energy QCD may be approached by other methods, as the solution of Schwinger-Dyson equations, QCD sum rules and effective models (for a review see, e.g., [1]). In particular, models inspired by the AdS/CFT correspondence [2–6] proved useful to describe different aspects of hadrons with various spins, as glueballs [7–25], as well as for mesons and baryons, as for instance, in [26–49].

The holographic hard wall (HW) model [14,15] introduces a hard cutoff in the anti–de Sitter (AdS) space, this way, hadronic masses M are proportional to the zeros of Bessel functions, $J_\nu(z)$, i.e., proportional to the value of the argument z where the corresponding Bessel function is zero. This model was inspired by holographic descriptions of hard scattering of glueballs [3] and deep inelastic scattering of hadrons [4], and it is very useful to obtain hadronic form factors, structure functions, parton distribution functions, etc. (see, e.g., [50,51]). It is important to mention that in the HW, the order of the Bessel function ν is related to the conformal dimension of the dual operator. For instance, for even spin S glueballs, it reads $\nu = S + 2$ [20,28]. Actually, in Ref. [20], approximate linear Regge trajectories, $J \times M^2$, for light even glueballs were obtained $\alpha(t = M^2) = (0.80 \pm 0.40) + (0.26 \pm 0.02)M^2$ and compared to a reasonable approximation to that of the soft pomeron $\alpha(t = M^2) = 1.08 + 0.25M^2$ [52–60]. A similar analysis within the HW was done for odd spin glueballs comparing their Regge trajectories with the odderon [22] and also for other hadrons with different spins [28,29].

A well-known drawback of the HW model is that it leads to nonlinear Regge trajectories. This problem is overcome by the soft wall model which has exact linear Regge trajectories [32]. This works very well for scalar and vector mesons [32,41] also reproducing masses of light states, but for glueballs, despite the linear trajectory, the mass spectra [21] is not in agreement with lattice data or other approaches.

*rafaelcosta@pos.if.ufrj.br, rc-fis@outlook.com
†boschi@if.ufrj.br, hboschi@gmail.com

TABLE I. Masses in GeV of the J^{++} glueball operators with even spins from lattice data [54–60]. In the last column we present average values. The numbers in parenthesis represent the uncertainties.

J^{PC}	[54]	[55]	[56]	[57]	[57]	[58]	[59]	[59]	[60]	Average
0^{++}	1.475(30)(65)	1.73(05)(08)	1.71(05)(08)	1.58(04)	1.48(07)	1.795(60)	1.417(30)	1.498(58)	1.653(26)	1.59(07)
2^{++}	2.15(03)(10)	2.400(25)(120)	2.39(03)(12)			2.620(50)	2.363(39)	2.384(67)	2.376(32)	2.38(09)
4^{++}	3.64(09)(16)								3.69(08)	3.67(17)
6^{++}	4.36(26)(20)									4.36(46)

TABLE II. Masses in GeV of the J^{++} glueball operators with even spins from the original HW, the original SW (SW1 and SW2), and the DASW models, with the corresponding deviations from the average lattice data presented in Table I. See the text for details. The masses of the 0^{++} state are inserted as inputs for the different models.

J^{PC}	HW	δ_{HW}	SW_1	δ_{SW1}	SW_2	δ_{SW2}	DASW	δ_{DASW}
0^{++}	1.59	0.0%	1.59	0.0%	2.83	78%	1.56	1.9%
2^{++}	2.35	1.3%	1.95	18%	3.46	45%	2.52	5.9%
4^{++}	3.08	16%	2.24	39%	4.00	9.0%	3.43	6.5%
6^{++}	3.78	13%	2.51	42%	4.47	2.5%	4.32	0.9%
8^{++}	4.48		2.75		4.90		5.19	
10^{++}	5.17		2.97		5.29		6.05	

See Tables I and II for comparisons. The soft wall (SW) model can be improved in many different ways and in particular if one considers dynamical corrections and anomalous dimensions the glueball spectra becomes good (see Table II), but it no longer has linear Regge trajectories [23,24].

In this work, we consider the inclusion of anomalous dimensions in the conformal dimension of boundary operators in the holographic HW model. As is well known [1], anomalous dimensions appear in QCD loop corrections, as in the Balitsky-Fadin-Kuraev-Lipatov (BFKL) pomeron [53], as well as in a semiclassical limit of gauge/string dualities [5]. As we show here, the introduction of anomalous dimensions in the HW model lead to improvements of the model allowing to match the Regge trajectory of the pomeron, $\alpha(t = M^2) = 1.08 + 0.25M^2$, also obtain good glueball masses when compared with lattice data, and better than the usual HW model. In particular, we show that considering the dimension Δ of the spin S operators as $\Delta = a\sqrt{S} + b$, where a and b are constants, implies asymptotic linear Regge trajectories associated with even glueballs.

This work is organized as follows. In Sec. II, we briefly review the AdS/CFT correspondence and the description of scalar fields in AdS space. In Sec. III we review the main properties of the original HW model which are relevant to the discussion of the anomalous HW model introduced in Sec. IV, with specific expressions for the anomalous dimensions starting with the logarithm case, truncated series, as a square root and a linear anomalous HW model. In Sec. V, we give the basic facts of the pomeron Regge trajectory and present detailed discussion of the models introduced in Sec. IV. In Sec. V A, we present three different fits for the logarithm anomalous dimensions adjusting the pomeron trajectory and predicting glueball masses compared with lattice data, and a fourth case fitting glueball masses and giving the Regge trajectory as an output. In Sec. V B, we present a series expansion of the logarithm anomalous dimensions an truncated approximations for it which we fit with the pomeron trajectory reproducing glueball masses. In Sec. V C, we present an even simpler expression for the anomalous dimension as a linear plus a square root of the spin of the glueball operator targeting the pomeron trajectory giving very good masses for glueball when compared with lattice data. In Sec. VI, inspired by the previous cases, we introduce an asymptotic linear anomalous HW model fitting very well the pomeron trajectory and present good glueball masses compared with lattice results. Finally, in Sec. VII, we present a summary of our results and our conclusions.

II. BRIEF REVIEW OF AdS/CFT AND SCALAR FIELDS IN AdS SPACE

Essentially, the AdS/CFT correspondence [2] is an equivalence between a superstring theory, formulated in a ten-dimensional spacetime, the $AdS_5 \times S^5$, and a super Yang-Mills field theory with conformal symmetry, which lives on the boundary of AdS_5, the four-dimensional Minkowski space. Here, AdS_5 is the five-dimensional anti–de Sitter spacetime, and S^5 the sphere in five dimensions. The space generated by this product of two manifolds is understood as follows: each point of AdS_5 is tangential to the sphere S^5.

A conformal theory in d spacetime dimensions is invariant by a set of transformations characterized by the

group $SO(2,d)$, including scale transformations as a particular case. Essentially, such transformations do not preserve lengths, but preserves angles.

Anti–de Sitter space is a space of constant negative curvature, while the sphere is a space of constant positive curvature. When inserted into a higher dimensional (pseudo-)Euclidean space, we can easily describe how its coordinates behave. Let X^μ be the coordinates of AdS_5, with $\mu \in (0,1,\ldots,5)$, and Y^a be the coordinates of S^5, with $a \in (1,2,\ldots,6)$. Such coordinates satisfy the following relations:

$$-(X^0)^2+(X^1)^2+(X^2)^2+(X^3)^2+(X^4)^2-(X^5)^2=-R^2,$$
$$(Y^1)^2+(Y^2)^2+(Y^3)^2+(Y^4)^2+(Y^5)^2+(Y^6)^2=R^2, \quad (1)$$

where R is a constant which plays the role of the radius of both the AdS_5 and the S^5 spaces.

Our aim here is to motivate the correspondence based on symmetry arguments. From the point of view of string theory, we have a ten-dimensional spacetime, formed by the direct product of two manifolds. The five-dimensional anti–de Sitter space has isometry described by the group of conformal transformations $SO(4,2)$. The five-dimensional sphere has $SO(6)$ as its isometry group.

The boundary theory living in Minkowski space has exactly the same isometries as the bulk theory with symmetry group $SO(4,2) \otimes SO(6)$. Then, the Minkowski field theory has conformal symmetry $SO(4,2)$ and it is supersymmetric with $\mathcal{N}=4$ supercharges. As a consequence, it presents R symmetry associated with the group $SU(4)$ that is isomorphic to $SO(6)$.

Based on these arguments, we see that the symmetries that arise in the two theories are the same. This is not enough to prove correspondence, but it is a strong indication that there is, in fact, a relationship between the two theories.

In fact, in 1973, Gerard 't Hooft presented [61] an approximate method to treat $SU(N)$ gauge theories with large N, with N being the number of colors in the theory. In this regime, the topological structures of the Feynman diagrams of field theory are identical to the topological structures of the diagrams in string theory. The 't Hooft parameter is given by

$$\lambda = g_{\mathrm{YM}}^2 N, \quad (2)$$

where g_{YM} is the Yang-Mills field theory coupling constant. Therefore, this parameter is directly related to the magnitude of the interaction. Later, the AdS/CFT correspondence would state that

$$\lambda = \frac{R^4}{\alpha'^2}, \quad (3)$$

where R is the radius of curvature of S^5 and α' is the slope parameter of string theory. Thus, we notice that for a fixed radius R, when we have small α', we have large g_{YM}, and vice versa. In this way, we have already noticed the power of correspondence, because, in nonperturbative regimes of field theory, where g_{YM} is large, string theory has small α', being weakly coupled and, therefore, easily treatable. Therefore, we can obtain information from a field theory in its nonperturbative regime through this duality.

The claim that a ten-dimensional string theory is dual to a four-dimensional field theory may initially seem strange. The idea is similar to holography, where a three-dimensional image is encoded entirely into a two-dimensional object. The Minkowski spacetime, being the boundary of the anti–de Sitter space, contains information from theories that propagate in AdS_5.

From the initial topics of modern physics, we know wave-particle duality. We can ask ourselves what the fundamental nature is, wave or particle. Today, we know that the answer is none of them, and what is understood is that both wave behavior and corpuscular behavior are classical limits of the theory, the Hilbert space of either description is the same. In the case of the AdS/CFT correspondence, the same occurs: the Hilbert space of string theory in $AdS_5 \times S^5$ is the same as that of conformal field theory in four-dimensional Minkowski.

Now, let us analyze a result that will be useful to us soon, the behavior of a scalar field in AdS_{d+1} [6]. Let us start by writing the metric of this space,

$$ds^2 = \frac{R^2}{z^2}(dz^2+\eta_{\mu\nu}dx^\mu dx^\nu), \quad (4)$$

where R is the AdS radius and $\eta_{\mu\nu}$ is the metric of the Minkowski space with coordinates $x^\mu=(x^0,x^1,\ldots,x^{d-1})$ defined on the d-dimensional boundary of the AdS space. So, the conformal border is obtained when we have $z=0$, plus an additional point at $z\to\infty$.

A scalar field ϕ with mass m in the space defined by the metric (4) is governed by the Klein-Gordon equation:

$$z^{d+1}\partial_z(z^{1-d}\partial_z\phi)+z^2\eta^{\mu\nu}\partial_\mu\partial_\nu\phi-(mR)^2\phi=0. \quad (5)$$

Let us then perform a Fourier transform of the field ϕ in the coordinates x^μ, that is,

$$\phi(z,x^\mu)=\int \frac{d^dk}{(2\pi)^d}e^{ik\cdot x}f_k(z). \quad (6)$$

In this way, the equation of motion becomes

$$z^{d+1}\partial_z(z^{1-d}\partial_z f_k)-k^2z^2f_k-(mR)^2f_k=0. \quad (7)$$

We are interested in its behavior near the frontier $z=0$. If we impose such a condition on the equation above, then we note that a natural solution is $f_k(z)\sim z^\beta$, with β satisfying

$$\beta(\beta - d) - (mR)^2 = 0, \tag{8}$$

so that

$$\beta = \frac{d}{2} \pm \sqrt{\frac{d^2}{4} + (mR)^2}. \tag{9}$$

Defining

$$\Delta \equiv \frac{d}{2} + \sqrt{\frac{d^2}{4} + (mR)^2}, \tag{10}$$

we have that, close to the border $z \sim 0$, the function $f_k(z)$ behaves as

$$f_k(z) \approx A(k) z^{d-\Delta} + B(k) z^{\Delta}. \tag{11}$$

We can then perform an inverse Fourier transform, in order to obtain the field close to the boundary ($z \to 0$) in the configuration space:

$$\phi(z, x) \approx A(x) z^{d-\Delta} + B(x) z^{\Delta}. \tag{12}$$

It is important to note that Δ is real if the term inside the root is greater than or equal to zero, that is,

$$m^2 \geq -\left(\frac{d}{2R}\right)^2, \tag{13}$$

which is known as the Breitenlohner-Freedman bound [62].

If the above condition is valid, we see that $d - \Delta \leq \Delta$. Thus, the term $z^{d-\Delta}$ is dominant as we approach $z = 0$. In order to have a finite field operator $\varphi(x)$ on the border we write

$$\varphi(x) = \lim_{z \to 0} z^{\Delta - d} \phi(z, x). \tag{14}$$

The corresponding action coupling $\phi(z, x)$ to a boundary operator $\mathcal{O}$ evaluated at $z \to \epsilon$ is the following

$$S_{\text{boundary}} \sim \int d^d x \sqrt{\gamma_\epsilon} \phi(\epsilon, x) \mathcal{O}(\epsilon, x), \tag{15}$$

where $\gamma_\epsilon = (R/\epsilon)^{2d}$ is the determinant of the induced metric at $z = \epsilon$. Then,

$$S_{\text{boundary}} \sim R^d \int d^d x \varphi(x) \epsilon^{-\Delta} \mathcal{O}(\epsilon, x). \tag{16}$$

To have a finite and ϵ-independent boundary action we define

$$\mathcal{O}(\epsilon, x) \equiv \epsilon^{\Delta} \mathcal{O}(x). \tag{17}$$

The above relationship shows us, therefore, that scalar excitations of the string, of mass m, couple to field operators on the boundary that have dimensions Δ. This result is extremely important in the analysis we will carry out to calculate hadron masses in the following.

III. THE ORIGINAL HW MODEL

The AdS/CFT correspondence alone will not allow us to calculate the masses of glueballs, once in a conformal field theory (CFT) physical quantities are massless. In the HW model [14,15] one considers the AdS metric given by Eq. (4) and introduces a cut in the holographic z coordinate imposing that $z \in [0, z_{\text{max}}]$, such that

$$z_{\text{max}} = \frac{1}{\Lambda_{\text{QCD}}}, \tag{18}$$

where Λ_{QCD} is a typical QCD mass scale with a value around 150–300 MeV.

As discussed in the previous section, from the AdS/CFT correspondence one is able to show that scalar excitations with mass m in AdS couple to scalar field operators at the boundary whose dimensionality is Δ, given by Eq. (10). Still, according to the correspondence a spin $J > 0$ field in AdS is equivalent to a massless spin J field operator on its border [2].

Phenomenologically, it was proposed that in the HW model the glueball operator with dimension Δ and nonzero spin couples to a massive scalar excitation in AdS according to [28]

$$\Delta = 2 + \sqrt{4 + (mR)^2}, \tag{19}$$

or

$$(mR)^2 = \Delta(\Delta + 4). \tag{20}$$

The scalar glueball operator on the boundary is given by $\mathcal{O}_4 = \text{tr} F_{\mu\nu}{}^a F^{\mu\nu a} \equiv \text{tr} F^2$ which has mass dimension $\Delta = 4$ and $F^a_{\mu\nu}$ is the usual Yang-Mills tensor with non-Abelian index $a \in (1, \ldots, N)$ of the $SU(N)$ gauge group. Following the idea [5] that high spin operators can be constructed by inserting covariant derivatives D_μ into lower spin operators one can write high spin S glueball operators as

$$\mathcal{O}_{4+S} = \text{tr} F D_{\{\mu_1} \ldots D_{\mu_S\}} F, \tag{21}$$

such that in four dimensions they have conformal dimension $\Delta = 4 + S$ [28]. Then, one has

$$\begin{aligned} 4 + S &= 2 + \sqrt{4 + (mR)^2}, \\ (S + 2)^2 &= 4 + (mR)^2, \\ (mR)^2 &= S(S + 4). \end{aligned} \tag{22}$$

This is a twist $\tau = 4$ tower of operators, since in general the twist is defined as $\tau = \Delta - S$. It is important to mention that these mass dimensions are all canonical:

$$\Delta_{\text{can}} = 4 + S. \tag{23}$$

Therefore, the equation of motion associated with glueballs in AdS_5 space, Eq. (5), becomes

$$\left[z^3\partial_z\frac{1}{z^3}\partial_z + \eta^{\mu\nu}\partial_\mu\partial_\nu - \frac{(mR)^2}{z^2}\right]\phi = 0. \tag{24}$$

Substituting the relation (22) in the above equation, one has

$$\left[z^3\partial_z\frac{1}{z^3}\partial_z + \eta^{\mu\nu}\partial_\mu\partial_\nu - \frac{S(S+4)}{z^2}\right]\phi = 0. \tag{25}$$

Taking a plane wave ansatz in $\vec{x}$ and in time t, that is,

$$\phi(x,z) = Ae^{-iP\cdot x}f(z), \tag{26}$$

and, substituting it into the equation of motion, one finds

$$\phi(x,z) = C_{\nu,k}e^{-iP\cdot x}z^2J_\nu(u_{\nu,k}z), \tag{27}$$

where $C_{\nu,k}$ are normalization constants that will not be important in our analysis, $J_\nu(u_{\nu,k}z)$ is the Bessel function of order $\nu = 2 + S$, $u_{\nu,k}$ $(k = 1, 2, \ldots)$ are discrete modes determined by boundary conditions. In this work we will impose Dirichlet boundary conditions, that is,

$$\phi(x,z)|_{z=z_{\max}} = 0, \tag{28}$$

which implies that

$$u_{\nu,k} = \frac{\chi_{\nu,k}}{z_{\max}} = \chi_{\nu,k}\Lambda_{\text{QCD}}, \qquad J_\nu(\chi_{\nu,k}) = 0. \tag{29}$$

The scale Λ_{QCD} is usually fixed using some experimental or lattice data. The k indices label the radial excitations of 3the particle states with masses proportional to the zeros of the Bessel function $J_\nu(w)$, i.e., proportional to the value of the argument w where the corresponding Bessel function is zero.

So, using the above discussion of the HW model, one can calculate higher spin glueball masses from relations (29) and (23) such that with $\nu = \Delta - 2 = S + 2$

$$u_{S+2,k} = \chi_{S+2,k}\Lambda_{\text{QCD}}. \tag{30}$$

Using this relation, one finds the glueball masses M_i from the original HW [20],

$$\frac{M_0}{\chi_{2,1}} = \frac{M_2}{\chi_{4,1}} = \frac{M_4}{\chi_{6,1}} = \cdots = \frac{M_i}{\chi_{i+2,1}} = \cdots, \tag{31}$$

which are presented here for latter convenience in Table II, and the corresponding relative deviations $\delta_i = |M_i - M_{\text{latt}}|/M_{\text{latt}}$ with respect to the average of lattice data presented in Table I. We use the mass of the 0^{++} glueball state from lattice as an input. For comparison, we also include the corresponding masses calculated from the SW model given by $m_J^2 = k[4 + 2\sqrt{4 + J(J+4)}] = 2k(J+4)$ with $k_1 = 0.316$ GeV^2 (SW1) and $k_2 = 1.00$ GeV^2 (SW2) [23], and the dynamical anomalous SW (DASW) model [24]. Despite the SW model providing a linear trajectory, as we can see, the masses obtained are not in good agreement with the masses obtained by lattice QCD. In the case where the masses presents small deviations (DASW), the Regge trajectory becomes nonlinear. This is a good reason to search for a possibility of linearity in HW model, since it could provide good masses combined with a linear Regge trajectory.

IV. ANOMALOUS HW MODELS

Before we introduce the anomalous HW model, let us briefly discuss the role of anomalous dimensions in quantum field theory. In a scale invariant field theory, such as a CFT, under a dilation $x \to \lambda x$ the operators $\mathcal{O}$ by definition behave as

$$\mathcal{O} \to \lambda^{-\Delta}\mathcal{O}, \tag{32}$$

where Δ is the conformal dimension of $\mathcal{O}$. In free field theories Δ is simply the mass dimension of the operator that can be read off directly from the Lagrangian by dimensional analysis. Nonetheless, for interacting field theories the renormalization process modifies this dimension according to

$$\Delta = \Delta_{\text{can}} + \gamma(g), \tag{33}$$

where Δ_{can} is the canonical conformal dimension of the operator in a free field theory, $\gamma(g)$ is the so-called anomalous dimension, and g is the running coupling of the theory. So, the anomalous dimension gives us a measure of the deviation of the conformal dimension from the value that it would assume in a free field theory.

It is clear that anomalous dimension becomes relevant when there is interaction in the theory. Therefore, it may not be obvious how it can emerge in the HW model, since for $z < z_{\max}$ the coupling constant seems to be null. Despite the fact that we are working with free theories in the AdS bulk, it is an approximation. As we can see in Eqs. (2) and (3), the string theory coupling constant α' and the coupling constant of the field theory in the boundary, g_{YM}, have a relation: when the first one becomes small, the second becomes big and vice versa. We are interested of treating the nonperturbative regime of QCD at the boundary (large g_{YM}), that implies a small (that we treat as zero in first approximation) α' at the bulk.

Even if the constant α' is treated as null, the operators that we are interested in have anomalous dimensions. The glueball operators, as evidenced by Eq. (21), are formed

by $F^a_{\mu\nu}$ and these last by elementary operators A^a_μ, that describes the $SU(N)$ gauge field. These are the operators that have their conformal dimension changed by interaction. At the boundary, the coupling constant of the theory $g_{\rm YM}$ assumes a finite value that implies an anomalous dimension for $F^a_{\mu\nu}$ and consequently, for the glueball operators.

Our proposal here, is to include anomalous dimensions in the conformal dimension of the boundary glueball operators, modifying the relation between Δ and S. It is well known that anomalous dimensions play a important role in the renormalization of QCD (see, e.g., [1]) and the BFKL pomeron [53]; however it is difficult to relate it to high spin states in field theory.

On the other hand, from a semiclassical limit of gauge/string dualities [5], one finds that the conformal dimension of dual operators with spins S, as the ones given by Eq. (21), behaves differently as one increases the spin S in comparison with the square root of the 't Hooft coupling λ. Basically, one finds three regimes:

(1) If the spins are small which means $S \ll \sqrt{\lambda}$, then the operators $\mathcal{O}$ have canonical conformal dimension

$$\Delta = 4 + S, \tag{34}$$

as in Eq. (23).

(2) If the spins are large as $S \gg \sqrt{\lambda}$, then

$$\Delta = S + \frac{\sqrt{\lambda}}{\pi}\ln\left(\frac{S}{\sqrt{\lambda}}\right) + \mathcal{O}(S^0), \tag{35}$$

so that the anomalous dimensions are given by

$$\Delta_{\rm anom} = \frac{\sqrt{\lambda}}{\pi}\ln\left(\frac{S}{\sqrt{\lambda}}\right) + \mathcal{O}(S^0). \tag{36}$$

(3) If the spins are of the same order of the square root of the 't Hooft coupling $S \sim \sqrt{\lambda}$, then some other unknown complicated nonperturbative relation between Δ and S should hold.

The phenomenological anomalous holographic HW model that we are proposing starts with the hard cutoff, Eq. (18), the equation of motion, Eq. (24), and the higher spin glueball masses are given by

$$\frac{M_0}{\chi_{2,1}} = \frac{M_i}{\chi_{\nu_i,1}}, \tag{37}$$

with the index of the Bessel function is given by $\nu_i = \Delta_{\rm AHW_i} - 2$, where $\Delta_{\rm AHW_i}$ takes into account the anomalous dimensions discussed above. The uncertainties in the masses are then:

$$\delta M_i = \sqrt{\left(\frac{\chi_{\nu_i,1}}{\chi_{2,1}}\right)^2(\delta M_0)^2 + \left(\frac{M_0}{\chi_{2,1}}\right)^2(\delta\chi_{\nu_i,1})^2}, \tag{38}$$

where the uncertainties δM_0 come from lattice data and $\delta\chi_{\nu_i,1}$ from the determination of the zero of the Bessel functions for high spins due to uncertainties in the anomalous dimensions to be discussed below. For low spins, we suppose the canonical dimension, Eq. (34), holds, in which case $\delta\chi_{\nu_i,1} = 0$, while for high spins the anomalous dimensions, Eq. (36), are assumed without an intermediate regime as follows:

$$\Delta_{\rm AHWlog} = \begin{cases} 4+S & 0 \le S \le S_0 \\ S + a\ln(S) + b & S > S_0 \end{cases}, \tag{39}$$

where the value of the spin S_0 of the transition between low ($0 \le S \le S_0$) and high ($S > S_0$) spins and the constants a and b will be determined by the best fit to experimental and lattice data. As we are going to see below in Sec. V A, this model produces interesting results, improving the ones from the usual HW and soft wall models regarding the predicted masses and from the HW with respect to the corresponding Regge trajectories.

Inspired by these results, we also consider other phenomenological anomalous HW models where we introduce some approximations for the anomalous dimensions for high spins. The first approximation we consider is motivated by truncated series expansions of the relation $\ln x = 2\text{arcsinh}[(1/2)(\sqrt{x} - 1/\sqrt{x})]$ leading to the models:

$$\Delta_{\rm ATSHW} = \begin{cases} 4+S, & 0 \le S \le S_0 \\ S + a\sum_{k=0}^{N}\frac{(-1)^k}{2^{2k}(2k+1)k!}\left(\frac{1}{2}\right)_k\left(\sqrt{S} - \frac{1}{\sqrt{S}}\right)^{2k+1} + b, & S > S_0 \end{cases}, \tag{40}$$

with $N = 0, 1, 2, 3$, discussed in Sec. V B from which we obtain good glueball masses and Regge trajectories.

Further, we consider another approximation leading to an AHW model with a square root anomalous dimension for high spins:

$$\Delta_{\rm AHWSQRT} = \begin{cases} 4+S, & 0 \le S \le S_0 \\ S + a\sqrt{S} + b, & S > S_0 \end{cases}, \tag{41}$$

presented in Sec. V C, which give very good results for glueball masses although not so good Regge trajectories.

Finally, we consider an even simpler expression for the anomalous dimension for high spins without the linear term S:

$$\Delta_{\mathrm{ALHW}} = \begin{cases} 4+S, & 0 \le S \le S_0 \\ a\sqrt{S}+b, & S > S_0 \end{cases}, \quad (42)$$

discussed in Sec. VI, which leads to good glueball masses and linear Regge trajectories in this AHW model.

V. GLUEBALLS AND THE SOFT POMERON IN THE AHW MODELS

The rise of the proton-proton cross section with energy is related to the soft pomeron, a particle with no charges and quantum numbers of the vacuum, whose experimental Regge trajectory is the following [52,54]:

$$\alpha(t = M^2) = 1.08 + 0.25M^2, \quad (43)$$

with masses M expressed in GeV. The BFKL pomeron [53] is a perturbative treatment of the problem, although nonperturbative aspects are also present (see, e.g., [63]).

In this work we analyze many possibilities of anomalous conformal dimensions for glueball operators and compare their masses with the masses of average lattice, presented in Table I. Despite we could use the best match with such masses of lattice as the criterion to determine the best model we are interested in a connection with the pomeron.

For that reason, our criterion of best fit is defined as follows: in a model, a given anomalous dimension produces some values for glueball masses. With these masses we use linear regression to obtain the corresponding Regge trajectory. The best fit is obtained when such Regge trajectory is as close as possible to the soft pomeron, given by Eq. (43), with smaller χ^2/ndf.

In all models considered in this work, we assume that the state 0^{++} has canonical conformal dimension $\Delta = 4$, and use it as an input with mass $M_{0^{++}} = 1.59$ GeV from lattice. Following Landshoff [52], we take that this state does not belong to the soft pomeron trajectory.

A. Logarithm anomalous dimensions

Here, we start with the AHWlog model

$$\Delta_{\mathrm{AHWlog}} = \begin{cases} 4+S & 0 \le S \le S_0 \\ \Delta_{\log} & S > S_0 \end{cases}, \quad (44)$$

where

$$\Delta_{\log} = S + a\ln(S) + b, \quad (45)$$

and the constants S_0, a, and b will determined fitting experimental and lattice data below. First, we consider that $0 \le S \le 10$ and $S_0 = 0$. The best fit obtained in this way implies the coefficients $a = 1.92 \pm 0.36$, and $b = 2.13 \pm 0.07$, such that the effective dimension in this anomalous HW model is given by

$$\Delta_{\log 1} = S + (1.92 \pm 0.36)\ln(S) + 2.13 \pm 0.07, \quad (2 \le S \le 10). \quad (46)$$

From this anomalous dimension, we obtain the glueball masses M_i shown in the second column of Table III with the corresponding errors given by Eq. (38), together with the deviations $\delta_i = |M_{\mathrm{latt}} - M_i|/M_{\mathrm{latt}}$ from average lattice data (Table I) and the effective anomalous dimensions of the glueball operators J^{++}. In Fig. 1, we present the Regge trajectory, which is built up as a linearization of these glueball masses, reproducing the soft pomeron trajectory, $J = 1.08 \pm 0.21 + (0.25 \pm 0.01)M^2$ with $\chi^2/\mathrm{ndf} = 3.76/3 = 1.25$. For clarity, we also show in Table III the order of the Bessel function for each glueball state in each AHWlog model.

The second case of the AHWlog model that we analyze is the one corresponding to $0 \le S \le 10$ and $S_0 = 2$. In this way, the states 0^{++} and 2^{++} have canonical conformal

TABLE III. Masses in GeV of the J^{++} glueball operators from $J = 0$ to $J = 10$ for the logarithm anomalous HW models ($\mathrm{HW}_{\log 1}$) and ($\mathrm{HW}_{\log 2}$) defined by Eq. (29) with the logarithm contributions to the anomalous dimensions Eqs. (46) and (47), respectively, with errors calculated according to Eq. (38). The orders ν of the corresponding Bessel functions are shown for each glueball state for the two models. The mass of the 0^{++} with uncertainties are inserted as inputs from lattice. We also show the relative deviations $\delta_{\log 1,2}$ compared with lattice data, and the corresponding anomalous dimensions $\Delta^{\log 1,2}_{\mathrm{anom}} \equiv \Delta_{\log 1,2} - (4+S)$ of the states J^{++} in this model.

J^{PC}	ν	$\mathrm{HW}_{\log 1}$	$\delta_{\log 1}$	$\Delta^{\log 1}_{\mathrm{anom}}$	ν	$\mathrm{HW}_{\log 2}$	$\delta_{\log 2}$	$\Delta^{\log 2}_{\mathrm{anom}}$
0^{++}	2	1.59 ± 0.07	0%	0.0	2	1.59 ± 0.07	0%	0.0
2^{++}	3.46	2.15 ± 0.12	9.71%	−0.54	4	2.35 ± 0.10	1.26%	0.0
4^{++}	6.79	3.36 ± 0.21	8.49%	0.79	6.50	3.25 ± 0.24	11.35%	0.50
6^{++}	9.57	4.33 ± 0.28	0.63%	1.57	9.44	4.29 ± 0.29	1.69%	1.44
8^{++}	12.12	5.21 ± 0.33		2.12	12.10	5.21 ± 0.34		2.10
10^{++}	14.55	6.04 ± 0.37		2.55	14.62	6.06 ± 0.37		2.62

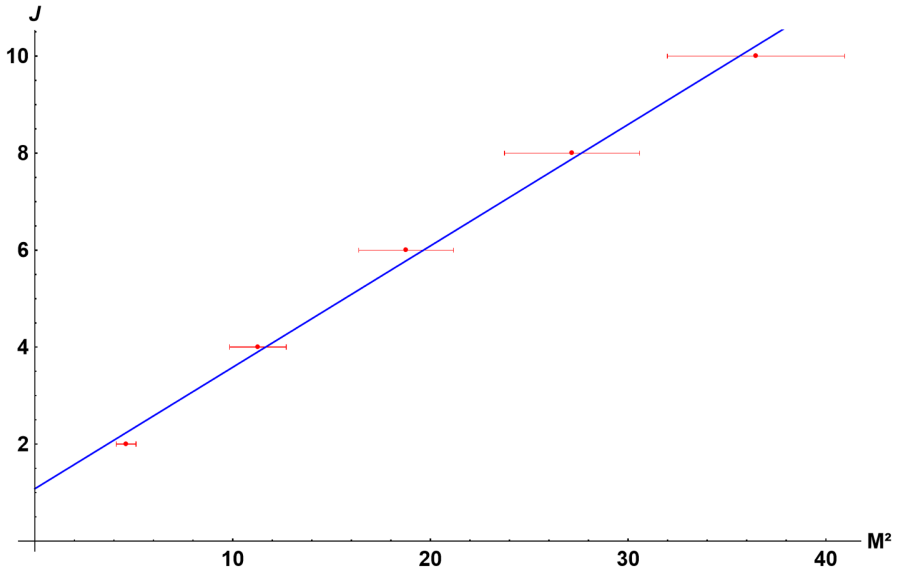

FIG. 1. Plot of $J \times M^2$ with masses expressed in GeV and $J = 2$ to 10 in the AHWlog model with anomalous dimensions given by Eq. (46). The dots represent the glueball masses shown in the second column of Table III with the corresponding error bars. The straight line corresponds to a linear fit of the soft pomeron trajectory $J = 1.08 \pm 0.21 + (0.25 \pm 0.01)M^2$ with $\chi^2/\text{ndf} = 3.76/3 = 1.25$.

dimensions $\Delta = 4$ and $\Delta = 6$, respectively, while higher spin states have anomalous dimensions given by Eq. (45). Applying this model to fit the pomeron trajectory and to obtain glueball masses for the states J^{++} from $J = 2$ to $J = 10$, we find that the best fit corresponds to

$$\Delta_{\log 2} = S + (2.32 \pm 0.25)\ln(S) + 1.28 \pm 0.21, \quad (4 \leq S \leq 10). \tag{47}$$

Within this AHWlog2 model we reobtain the soft pomeron trajectory $J = 1.08 \pm 0.36 + (0.25 \pm 0.02)M^2$, which is shown in Fig. 2, with $\chi^2/\text{ndf} = 15.2/3 = 5.1$. The glueball masses are presented in the fifth column of Table III with the corresponding errors given by Eq. (38), together with the deviations with respect to average lattice data and the corresponding anomalous dimensions of the states J^{++} in this model.

Third, we consider the AHWlog model with $0 \leq S \leq 10$ and $S_0 = 4$, so that the states 0^{++}, 2^{++}, and 4^{++} have canonical conformal dimensions, whilst higher spins follow Eq. (45). In this case it is not possible the match the soft pomeron trajectory exactly. The closest trajectory found with least χ^2 is $J = 1.10 \pm 0.47 + (0.27 \pm 0.02)M^2$, with $\chi^2/\text{ndf} = 24.6/3 = 8.2$ and effective dimension

$$\Delta_{\log 3} = S + (2.34 \pm 0.04)\ln(S) + 0.51 \pm 0.02, \quad (6 \leq S \leq 10), \tag{48}$$

starting with the state 6^{++}, implying masses $\{2.35 \pm 0.10, 3.08 \pm 0.14, 4.06 \pm 0.18, 4.96 \pm 0.22, 5.82 \pm 0.26\}$ GeV for the states from $J = 2$ to $J = 10$, with relative deviations $\{1.3, 16, 7.5\}\%$ compared with average lattice for the states 2^{++}, 4^{++}, and 6^{++}, respectively.

A comparison between the above three fits within the AHWlog model favors the first with respect to second and the third since it gives least χ^2 and χ^2/ndf. In the same token, the second AHWlog is better than the third, thanks to smaller χ^2 and χ^2/ndf.

Another possible way to apply the AHWlog model with logarithm anomalous dimensions is to minimize directly the deviations of the glueball masses with respect to average lattice data and then look up for the resulting Regge trajectory. We consider this case for $0 \leq S \leq 10$ and $S_0 = 0$, such that the state 0^{++} has canonical dimension $\Delta = 4$ and the higher spins from $J = S = 2$ to 10 have anomalous dimension given by Eq. (45). Applying this procedure one finds the coefficients $a = 2.3 \pm 0.8$ and $b = 2.5 \pm 1.1$, which means an effective dimension

$$\Delta_{\log 4} = S + (2.3 \pm 0.8)\ln(S) + 2.5 \pm 1.1, \quad (2 \leq S \leq 10), \tag{49}$$

obtaining exactly the average lattice masses for the 2^{++} and 4^{++} states besides the input 0^{++}. For the state 6^{++}, we find $M_{6^{++}} = 4.69$ GeV which is 7.6% higher than the average lattice result. So, this model produces masses with lowest total relative deviation with respect to average lattice outputs when compared with the AHWlog models discussed above. Within this model the predicted soft pomeron trajectory is not so good and is given by $J = 0.93 \pm 0.18 + (0.22 \pm 0.01)M^2$ with $\chi^2/\text{ndf} = 0.705/3 = 0.235$. If we want to compare this model with others, then we should compute χ^2 based on soft pomeron trajectory instead, by doing this we find $\chi^2/\text{ndf} = 5.62/3 = 1.87$.

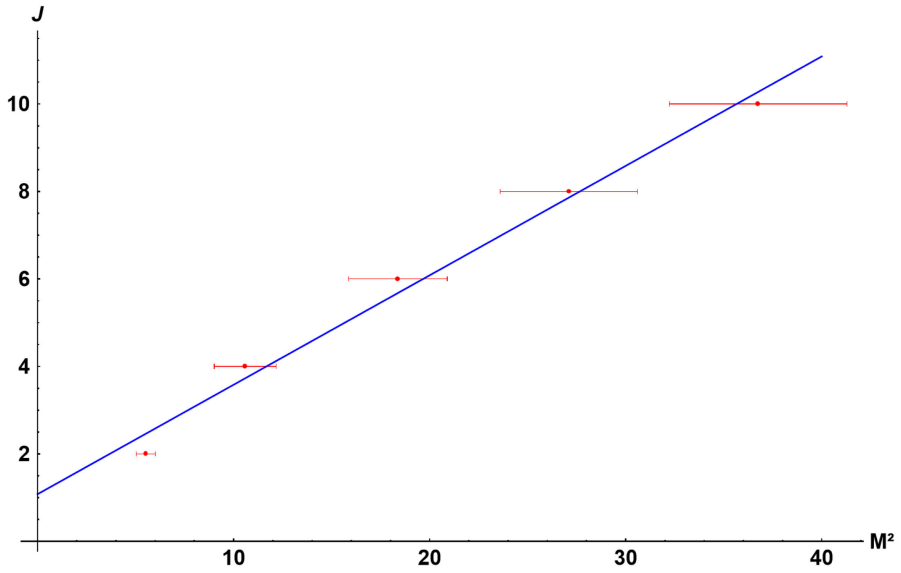

FIG. 2. Plot of $J \times M^2$ with masses expressed in GeV and $J = 2$ to 10 in the anomalous model $\mathrm{HW}_{\log 2}$, Eq. (47). The dots represent the glueball masses shown in the fifth column of Table III with the corresponding error bars. The straight line corresponds to a linear fit matching the soft pomeron trajectory $J = 1.08 \pm 0.36 + (0.25 \pm 0.02)M^2$ with $\chi^2/\mathrm{ndf} = 15.2/3 = 5.1$.

B. Truncated series for anomalous dimensions

The conformal dimension for high spins from gauge/string duality discussed in the previous section was developed to describe an ideal situation where the four-dimensional field theory is conformal. Since this is not the case of strong interactions that lead to the Regge trajectory of the soft pomeron and to the lattice glueball masses, it is also interesting to investigate some approximate expressions for this quantity since we are studying a phenomenological model, and analyze whether these expressions might give better results compared with experimental and lattice data.

Here, we start with the identity

$$\ln x = 2\mathrm{arcsinh}\left[\frac{1}{2}\left(\sqrt{x} - \frac{1}{\sqrt{x}}\right)\right], \tag{50}$$

which can be expanded for small x as

$$\begin{aligned}\ln x &= \sqrt{x} - \frac{1}{\sqrt{x}} - \frac{1}{24}\left(\sqrt{x} - \frac{1}{\sqrt{x}}\right)^3 + \frac{3}{640}\left(\sqrt{x} - \frac{1}{\sqrt{x}}\right)^5 \\ &\quad + \cdots, \\ &= \sum_{k=0}^{\infty} \frac{(-1)^k}{2^{2k}(2k+1)k!}\left(\frac{1}{2}\right)_k \left(\sqrt{x} - \frac{1}{\sqrt{x}}\right)^{2k+1},\end{aligned} \tag{51}$$

where $(\frac{1}{2})_k$ are the Pochhammer symbols of order k with argument $1/2$, the first values are $(\frac{1}{2})_0 = 1$, $(\frac{1}{2})_1 = \frac{1}{2}$, $(\frac{1}{2})_2 = \frac{3}{4}$, $(\frac{1}{2})_3 = \frac{15}{8}$, …. Using this expression one can rewrite the effective dimension (45) as

$$\Delta = S + a\sum_{k=0}^{\infty} \frac{(-1)^k}{2^{2k}(2k+1)k!}\left(\frac{1}{2}\right)_k \left(\sqrt{S} - \frac{1}{\sqrt{S}}\right)^{2k+1} + b. \tag{52}$$

Now, truncating the series at some finite value of $k = 0, 1, 2, 3, \ldots$, which means truncating at odd powers $2k+1$ of the difference $\sqrt{S} - 1/\sqrt{S}$, we obtain approximate expressions for Δ from which we can fit the soft pomeron trajectory and compare the obtained glueball masses with those from lattice calculations. Explicitly, we define this truncated effective dimension of high spin operators as

$$\Delta_N = S + a\sum_{k=0}^{N} \frac{(-1)^k}{2^{2k}(2k+1)k!}\left(\frac{1}{2}\right)_k \left(\sqrt{S} - \frac{1}{\sqrt{S}}\right)^{2k+1} + b. \tag{53}$$

Then, this anomalous truncated series HW model is characterized by the conformal dimension

$$\Delta_{\mathrm{ATSHW}} = \begin{cases} 4 + S, & 0 \le S \le S_0 \\ \Delta_N, & S > S_0 \end{cases}, \tag{54}$$

with Δ_N given by Eq. (53). Here, we choose $S_0 = 0$ and $0 \le S \le 10$, such that the conformal dimension for the 0^{++} state is $\Delta = 4$ and Eq. (53) give the effective dimension for the states 2^{++} up to 10^{++} truncated at N with $N = 0, 1, 2, 3$. Within this model, we successfully match the soft pomeron trajectory, $J = 1.08 + 0.25M^2$, in the four cases $N = 0, 1, 2, 3$. Details of the fits are presented in Table IV, together with the corresponding glueball masses and errors, the

TABLE IV. Masses of the J^{++} glueball operators in GeV from $J = 0$ to $J = 10$, with errors calculated according to Eq. (38), from the anomalous HW model Eq. (54) considering the approximate conformal dimension Eq. (53), truncating the series at $N = 0, 1, 2, 3$, with the corresponding deviations with respect to lattice data, and the anomalous dimensions $\Delta^N_{\text{anom}} \equiv \Delta_N - (4 + S)$ of the states in this model for each value of N. The mass of the 0^{++} is inserted as an input from lattice.

	$N = 0$			$N = 1$			$N = 2$			$N = 3$		
α_0	1.08 ± 0.28			1.08 ± 0.04			1.08 ± 0.34			1.08 ± 0.29		
α'	0.25 ± 0.01			0.250 ± 0.002			0.25 ± 0.02			0.25 ± 0.01		
$\chi^2/3$	1.74			0.104			2.19			1.07		
a	1.38 ± 0.26			2.86 ± 0.52			1.40 ± 0.26			3.49 ± 0.61		
b	2.67 ± 0.04			1.00 ± 0.26			2.82 ± 0.06			0.10 ± 0.38		
J^{PC}	M	δ_N	Δ^N_{anom}	M	δ_N	Δ^N_{anom}	M	δ_N	Δ^N_{anom}	M	δ_N	Δ^N_{anom}
0^{++}	1.59 ± 0.07	0%	0.0	1.59 ± 0.07	0%	0.0	1.59 ± 0.07	0%	0.0	1.59 ± 0.07	0%	0.0
2^{++}	2.22 ± 0.13	6.7%	−0.36	1.97 ± 0.09	17%	−1.03	2.27 ± 0.13	4.6%	−0.21	1.80 ± 0.08	24%	−1.47
4^{++}	3.34 ± 0.21	9.0%	0.74	3.39 ± 0.22	7.6%	0.87	3.35 ± 0.21	8.7%	0.77	3.41 ± 0.23	7.1%	0.94
6^{++}	4.30 ± 0.27	1.4%	1.49	4.42 ± 0.29	1.4%	0.81	4.28 ± 0.27	1.8%	1.41	4.56 ± 0.31	4.6%	2.22
8^{++}	5.20 ± 0.33		2.08	5.26 ± 0.33		2.25	5.17 ± 0.32		2.00	5.40 ± 0.36		2.69
10^{++}	6.05 ± 0.38		2.60	5.98 ± 0.36		2.37	6.08 ± 0.38		2.68	5.87 ± 0.34		2.07

associated deviations with respect to average lattice data and the values of the anomalous dimensions for each state. Analyzing these results, we see that the cases $N = 0$ and $N = 2$ present the smaller relative deviations with respect to average lattice output. We understand this behavior since the truncations at $N = 0$ and $N = 2$ contribute positively to the anomalous dimension (53) in contrast to the cases $N = 1$ and $N = 3$, once they come from an alternate series. In particular, the plots corresponding to the masses found from the approximate anomalous effective dimension (53), truncated at $N = 0$ and $N = 1$ are presented in Figs. 3 and 4, respectively, with the corresponding pomeron trajectories.

C. Square root anomalous dimension

Here, we consider another phenomenological anomalous HW model inspired by Eq. (53) for the anomalous dimension of the glueball operator with high spins. Considering the truncation of this equation at $N = 0$, and a further approximation we write the effective dimension as

$$\Delta_{\text{AHWSQRT}} = \begin{cases} 4 + S, & 0 \le S \le S_0 \\ \Delta_{\text{SQRT}}, & S > S_0 \end{cases}, \tag{55}$$

where

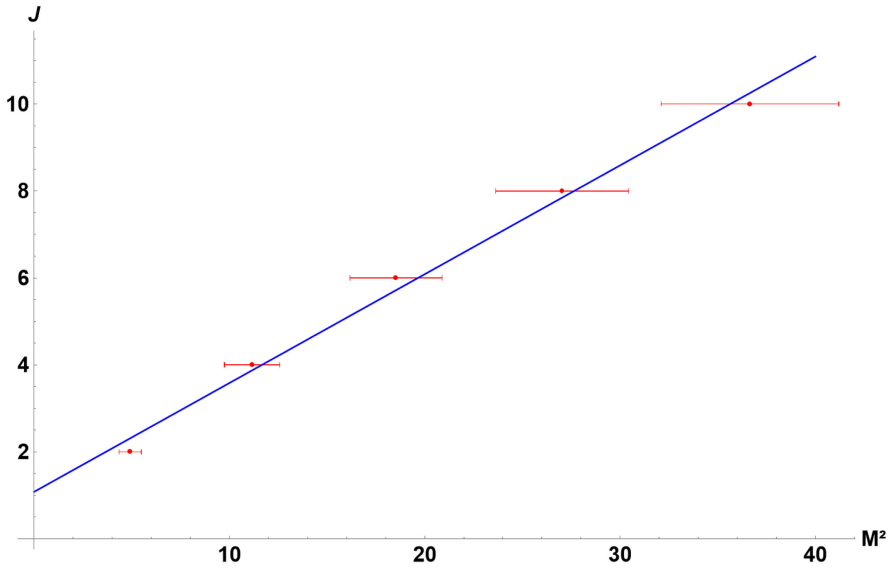

FIG. 3. Plot of $J \times M^2$ with masses M expressed in GeV and $J = 2$ to 10, using the anomalous HW model (54) with conformal dimension Eq. (53), truncated at $N = 0$ with coefficients $a = 1.38$ and $b = 2.67$. The dots with error bars represent the glueball masses shown in Table IV for $N = 0$, and the straight line corresponds to a linear fit given by $J = 1.08 \pm 0.28 + (0.25 \pm 0.01)M^2$ with $\chi^2/\text{ndf} = 5.21/3 = 1.74$.

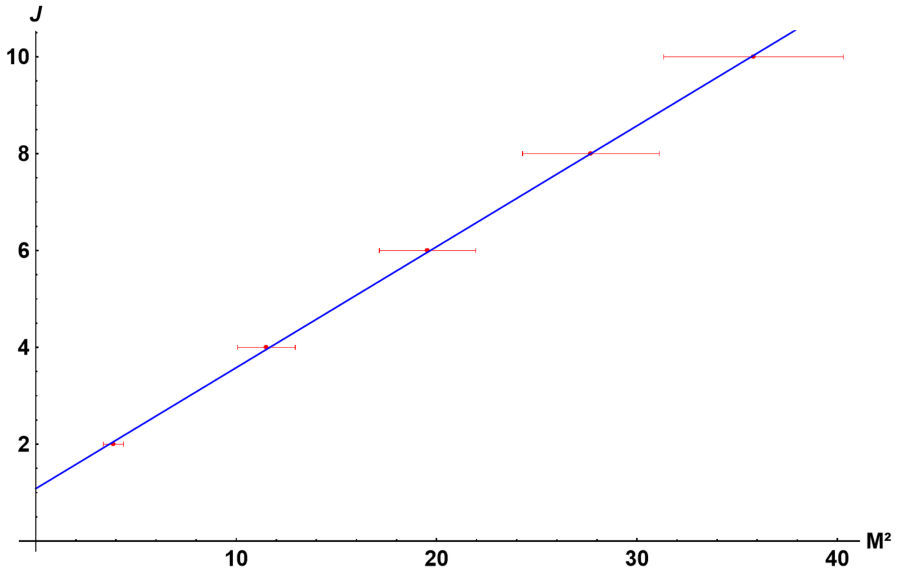

FIG. 4. Plot of $J \times M^2$ with M expressed in GeV and $J = 2$ to 10, using the approximate anomalous dimension Eq. (53), truncated at $N = 1$ with $a = 2.86$, $b = 1.00$. The dots with error bars represent the glueball masses shown in Table IV for $N = 1$, and the straight line corresponds to a linear fit given by $J = 1.08 \pm 0.04 + (0.250 \pm 0.002)M^2$ with $\chi^2/\text{ndf} = 0.312/3 = 0.104$.

$$\Delta_{\text{SQRT}} = S + a\sqrt{S} + b, \tag{56}$$

which represent square root anomalous dimensions. Here we choose $S_0 = 0$ and $0 \leq S \leq 10$. The above approximation for Δ_{SQRT} can be justified once we are applying this formula for spins S from 2 to 10 and the correction from the inverse square root is small in this range. Using this expression for the effective dimension of the glueball operators starting with $S = 2$, and minimizing the resulting linear trajectory for the corresponding glueball masses, we find the coefficients $a = 1.50 \pm 0.27$, $b = 2.0 \pm 0.12$. The obtained glueball masses with errors are listed in Table V, together with the relative deviations with respect to average lattice data and the associated anomalous dimensions for each J^{++} state. The linear coefficient of the resulting Regge trajectory, $J = 0.90 \pm 0.30 + (0.25 \pm 0.01)M^2$ with $\chi^2/\text{ndf} = 4.24/3 = 1.42$, is poorer than the corresponding ones from Eq. (53) shown in Table IV which match the soft pomeron trajectory, $J = 1.08 + 0.25M^2$. However it is remarkable that this simple model defined by Eq. (55) produces masses that have smaller relative deviations with respect to average lattice data in comparison with the results of Tables III and IV.

TABLE V. Masses of the J^{++} glueball operators in GeV from $J = 0$ to $J = 10$, with errors calculated according to Eq. (38), from the anomalous HW model, Eq. (55), with square root anomalous dimensions Δ_{SQRT} from Eq. (56), together with the corresponding errors and relative deviations δ_{SQRT} with respect to average lattice data, and the anomalous dimensions $\Delta^{\text{SQRT}}_{\text{anom}} \equiv \Delta_{\text{SQRT}} - (4 + S)$ of the states J^{++} in this case. The orders ν of the corresponding Bessel functions are shown for each glueball and the mass of the 0^{++} with uncertainties are inserted as inputs from lattice.

J^{PC}	ν	M_{SQRT}	δ_{SQRT}	$\Delta^{\text{SQRT}}_{\text{anom}}$
0^{++}	2	1.59 ± 0.07	0%	0.0
2^{++}	4.12	2.40 ± 0.14	0.8%	0.12
4^{++}	7.00	3.44 ± 0.21	6.3%	1.00
6^{++}	9.67	4.38 ± 0.27	0.5%	1.67
8^{++}	12.24	5.27 ± 0.32		2.24
10^{++}	14.74	6.12 ± 0.37		2.74

VI. ANOMALOUS LINEAR HW MODEL

In this section we consider another anomalous HW model inspired by the results of the previous sections. Our goal here is to obtain an asymptotic linear Regge trajectory from such a model. In this regard, we note that the linear dependence on the spin S in the effective dimension $\Delta = S + \frac{\sqrt{\lambda}}{\pi}\ln(\frac{S}{\sqrt{\lambda}}) + \mathcal{O}(S^0)$, Eq. (35), leads to parabolic Regge trajectories characteristic of the usual HW model. Then, the natural guess is to remove this linear dependence from a phenomenological effective dimension and try something of the form $\Delta = a\ln(S) + b$, but this does not lead to linear Regge trajectories too. The solution is to consider an effective dimension as

$$\Delta_{\sqrt{S}} = a\sqrt{S} + b. \tag{57}$$

So, the anomalous linear HW model is defined by

$$\Delta_{\text{ALHW}} = \begin{cases} 4 + S, & 0 \leq S \leq S_0 \\ \Delta_{\sqrt{S}}, & S > S_0 \end{cases}, \tag{58}$$

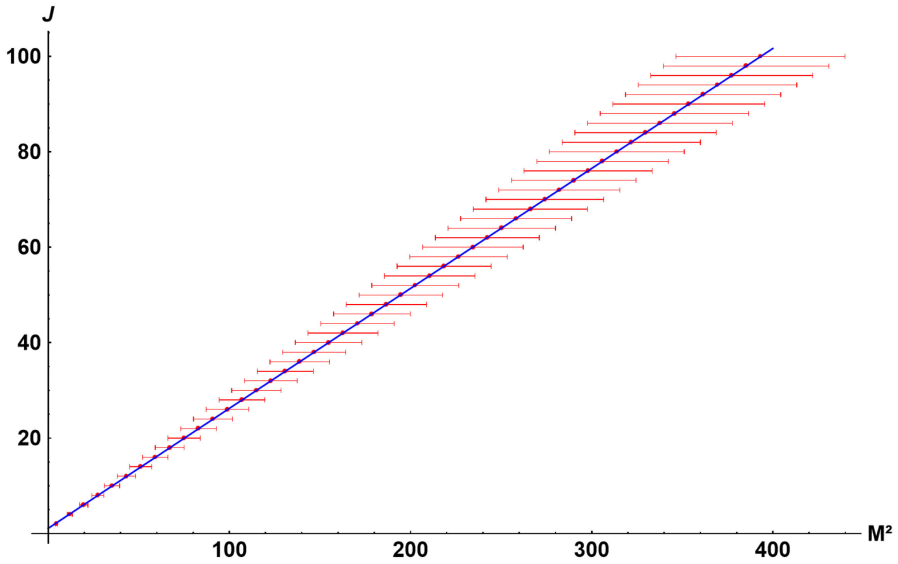

FIG. 5. Regge trajectory $J \times M^2$ for the anomalous linear HW model defined by Eq. (58), with $S_0 = 0$ and $0 \leq S \leq 100$. The dots with error bars represent the glueball masses obtained from this equation and their values corresponding to states from $J = 2$ to $J = 10$ are shown in Table VI. The straight line is the corresponding linear fit in the range from $J = 2$ to $J = 100$, matching the soft pomeron trajectory with a very precise angular coefficient, $J = 1.08 \pm 0.01 + (0.25144 \pm 0.00006)M^2$ with $\chi^2/\text{ndf} = 2.58/48 = 0.054$.

where $\Delta_{\sqrt{S}}$ is given by Eq. (57), and the constants S_0, a, and b will be fixed by best fit to experimental and lattice data. In order to check the possible linearity of this proposal we need to go to very high spin values. We choose $S_0 = 0$ and $0 \leq S \leq 100$. The best fit for the soft pomeron trajectory from $S = 2$ to 100 with this expression is obtained for $a = 6.20 \pm 0.26$, and $b = -3.35 \pm 0.11$, such that the effective dimension reads

$$\Delta_{\sqrt{S}} = (6.20 \pm 0.26)\sqrt{S} - 3.35 \pm 0.11. \tag{59}$$

The resulting trajectory is plotted in Fig. 5, and is in perfect agreement with the experimental soft pomeron trajectory, $J = 1.08 \pm 0.01 + (0.25144 \pm 0.00006)M^2$ with $\chi^2/\text{ndf} = 2.58/48 = 0.054$. The masses for glueballs obtained from this effective dimension are shown in Table VI, together with the relative deviations with respect to average lattice data, and the corresponding anomalous dimensions of the states J^{++}.

TABLE VI. Masses of the J^{++} glueball operators in GeV from $J = 0$ to $J = 10$ within the anomalous linear HW (ALHW) model, Eq. (58), with errors calculated according to Eq. (38). The orders ν of the corresponding Bessel functions are shown for each glueball state and the mass of the 0^{++} with uncertainties are inserted as inputs from lattice. We also show the relative deviations δ_{ALHW} compared with average lattice data, and the anomalous dimensions $\Delta^{\text{ALHW}}_{\text{anom}} \equiv \Delta_{\text{anom}} - (4 + S)$ of the glueball operators J^{++} in this model.

J^{PC}	ν	M_{ALHW}	δ_{ALHW}	$\Delta^{\text{ALHW}}_{\text{anom}}$
0^{++}	2	1.59 ± 0.07	0%	0.0
2^{++}	3.42	2.14 ± 0.13	10.1%	−0.58
4^{++}	7.05	3.46 ± 0.21	5.72%	1.05
6^{++}	9.84	4.44 ± 0.27	1.83%	1.84
8^{++}	12.19	5.96 ± 0.31		2.19
10^{++}	14.26	6.59 ± 0.35		2.26

Comparing the above results with the ones from Eq. (53), one may wonder whether a contribution of the inverse of the square root of S would spoil the linearity just found. Actually, considering a model with effective dimension given by $\Delta_{\tilde{N}=0} = a(\sqrt{S} - 1/\sqrt{S}) + b$ without the linear term, it is possible to obtain an asymptotic linear Regge trajectory in this case. Fitting the states from $J = 2$ to $J = 10$ with coefficients $a = 5.40 \pm 0.26$ and $b = 0.86 \pm 0.04$, we also match exactly the soft pomeron Regge trajectory in very good approximation, $J = 1.08 \pm 0.05 + (0.252 \pm 0.002)M^2$ with $\chi^2/\text{ndf} = 0.260/3 = 0.087$. The masses obtained for these states are $\{1.85 \pm 0.12, 3.42 \pm 0.21, 4.44 \pm 0.28, 5.25 \pm 0.33, 5.93 \pm 0.37\}$ GeV, with relative deviations $\{22.3, 6.81, 1.83\}$% with respect to average lattice data. This suggests that the results obtained from Eq. (59) are better. The other powers $N = 1, 2, 3$ of the difference $\sqrt{S} - 1/\sqrt{S}$ discussed in the previous section do not lead to asymptotic linear trajectories when high spins are considered, since they grow with $S^{(2N+1)/2}$.

VII. SUMMARY AND CONCLUSIONS

A. AHW models

In this work we propose anomalous HW models in four different formulations where we modify the conformal dimension for high spins S operators by introducing

anomalous dimensions inspired by a semiclassical limit of gauge/string dualities. For low spins the dimension of the spin operators are conformal ($\Delta = S + 4$) as in the original HW model. For high spins, these operators acquire anomalous dimensions in the form of a logarithm of S. Disregarding a complicated intermediate nonperturbative spin dependence, we take these results as a prescription to build up anomalous HW models. In general, to compare these models with experimental and lattice data, we adopt the strategy of first fitting the pomeron trajectory predicting glueball masses to be compared with lattice data. The effective dimensions of these four formulations of the anomalous HW models are as follows:

(1) Logarithm AHW

$$\Delta_{\mathrm{AHWlog}} = \begin{cases} 4 + S, & 0 \le S \le S_0 \\ S + a\ln(S) + b, & S > S_0 \end{cases}. \quad (60)$$

(2) Truncated series AHW

$$\Delta_{\mathrm{ATSHW}} = \begin{cases} 4 + S, & 0 \le S \le S_0 \\ \Delta_N, & S > S_0 \end{cases}, \quad (61)$$

where

$$\Delta_N = S + a\sum_{k=0}^{N} \frac{(-1)^k}{2^{2k}(2k+1)k!}\left(\frac{1}{2}\right)_k \times \left(\sqrt{S} - \frac{1}{\sqrt{S}}\right)^{2k+1} + b. \quad (62)$$

(3) Square root AHW

$$\Delta_{\mathrm{AHWSQRT}} = \begin{cases} 4 + S, & 0 \le S \le S_0 \\ S + a\sqrt{S} + b, & S > S_0 \end{cases}. \quad (63)$$

(4) Linear AHW

$$\Delta_{\mathrm{ALHW}} = \begin{cases} 4 + S, & 0 \le S \le S_0 \\ a\sqrt{S} + b, & S > S_0 \end{cases}. \quad (64)$$

B. Log models

In Sec. V A, we consider the specific case of logarithm anomalous dimensions, Eq. (60), where we study some numerical fits to reobtain the soft pomeron trajectory and even glueball masses for the states $J = 2$ to $J = 10$. In particular, in this section we analyze four different fits with the following phenomenological anomalous dimensions with the corresponding spins interval for which these expressions apply:

$$\Delta_{\log 1} = S + (1.92 \pm 0.36)\ln(S) + 2.13 \pm 0.07, \quad (2 \le S \le 10), \quad (65)$$

$$\Delta_{\log 2} = S + (2.32 \pm 0.25)\ln(S) + 1.28 \pm 0.21, \quad (4 \le S \le 10), \quad (66)$$

$$\Delta_{\log 3} = S + (2.34 \pm 0.04)\ln(S) + 0.51 \pm 0.02, \quad (6 \le S \le 10), \quad (67)$$

$$\Delta_{\log 4} = S + (2.3 \pm 0.8)\ln(S) + 2.5 \pm 1.1, \quad (2 \le S \le 10). \quad (68)$$

In the first three log anomalous dimensions, we follow the procedure of fitting the pomeron trajectory and then compare the glueball mass outputs with lattice data. In the fourth case we reverse this approach and fit the lattice masses and then compare the resulting Regge trajectory with that of the pomeron. With the first two fits we could reproduce precisely the pomeron trajectory $J = 1.08 + 0.25M^2$, while the third we found $J = 1.10 + 0.27M^2$. Actually, in the first fit we found better results regarding the deviations from the pomeron trajectory and smaller χ^2/ndf. In the fourth log fit we found good masses as expected but a poorer Regge trajectory $J = 0.93 + 0.22M^2$ when compared with the pomeron. The first two log fits also present better results for the pomeron trajectory and glueball masses than the original HW and SW models.

C. Truncated series models

In Sec. V B we discuss approximations to the logarithm anomalous dimensions in the form of an infinite series of odd powers of $(\sqrt{S} - 1/\sqrt{S})^{2N+1}$, which are truncated at $N = 0, 1, 2, 3$, as shown in Eq. (61). In these four cases they all fit the pomeron trajectory $J = 1.08 + 0.25M^2$ with different precisions. Regarding the glueball masses predictions when compared with lattice data, the cases with $N = 0$ and $N = 2$ present smaller relative deviations than the cases $N = 1$ and $N = 3$. In particular, for $N = 0, 1, 2$ the total relative deviations are smaller than that of the original HW model, while for $N = 3$ they are of the same order of magnitude. These results are also better than that of the original SW model.

D. Square root anomalous dimensions

Inspired by the results of the truncated series AHW models, in Sec. V C we discuss an AHW model with square root anomalous dimensions, Eq. (63). This model gives as output the Regge trajectory $J = 0.90 + 0.25M^2$, which does not fit exactly the soft pomeron. On the other hand, the predicted glueball masses by this model presents smaller deviations with respect to lattice data than the models with truncated series and the logarithm models

$\mathrm{AHW}_{\log 1}$, $\mathrm{AHW}_{\log 2}$, and $\mathrm{AHW}_{\log 3}$. Naturally, the glueball masses predicted by this model are much better than the ones from the original HW and SW models when compared with lattice data.

E. Anomalous linear HW model

In Sec. VI, we propose an anomalous linear HW model, Eq. (64), leading to asymptotic linear Regge trajectories even for very high spins ($J = 100$). In contrast, the original HW model is well known for producing nonlinear Regge trajectories. The main modification introduced in the linear model is that we take the dimension of the glueball operators $\Delta = a\sqrt{S} + b$ without the linear term S present in all anomalous models discussed above and also in the original HW model. The obtained Regge trajectory in the linear AHW model fits the soft pomeron with very high precision $J = 1.08 \pm 0.01 + (0.25144 \pm 0.00006)M^2$ with $\chi^2/\mathrm{ndf} = 2.58/48 = 0.054$, and the glueball masses compare well to lattice data with total deviation of the order of some above anomalous HW models, better than the original HW and SW models.

F. Conclusions

In conclusion, the anomalous HW models presented here show a significant improvement with respect to the original HW model in general and with respect to the original SW model regarding glueball spectra and the pomeron trajectory. This procedure of modifying the HW model with the inclusion of anomalous dimensions might be useful for other hadrons as mesons and baryons. This is presently under investigation.

ACKNOWLEDGMENTS

We would like to thank an anonymous referee for the criticisms and suggestions raised which helped us improve the quality of this work, especially in its numerical analysis. R. A. C.-S. is supported by Conselho Nacional de Desenvolvimento Científico e Tecnológico (CNPq) and Coordenação de Aperfeiçoamento de Pessoal de Nível Superior (CAPES) under finance code 001. H. B.-F. is partially supported by Conselho Nacional de Desenvolvimento Científico e Tecnológico (CNPq) under Grants No. 311079/2019-9 and No. 310346/2023-1.

[1] F. Gross, E. Klempt, S. J. Brodsky, A. J. Buras, V. D. Burkert, G. Heinrich, K. Jakobs, C. A. Meyer, K. Orginos, M. Strickland *et al.*, 50 years of quantum chromodynamics, Eur. Phys. J. C **83**, 1125 (2023).
[2] O. Aharony, S. S. Gubser, J. M. Maldacena, H. Ooguri, and Y. Oz, Large N field theories, string theory and gravity, Phys. Rep. **323**, 183 (2000).
[3] J. Polchinski and M. J. Strassler, Hard scattering and gauge/string duality, Phys. Rev. Lett. **88**, 031601 (2002).
[4] J. Polchinski and M. J. Strassler, Deep inelastic scattering and gauge/string duality, J. High Energy Phys. 05 (2003) 012.
[5] S. S. Gubser, I. R. Klebanov, and A. M. Polyakov, A semiclassical limit of the gauge/string correspondence, Nucl. Phys. **B636**, 99 (2002).
[6] A. V. Ramallo, Introduction to the AdS/CFT correspondence, Springer Proc. Phys. **161**, 411 (2015).
[7] C. Csaki, H. Ooguri, Y. Oz, and J. Terning, Glueball mass spectrum from supergravity, J. High Energy Phys. 01 (1999) 017.
[8] R. de Mello Koch, A. Jevicki, M. Mihailescu, and J. P. Nunes, Evaluation of glueball masses from supergravity, Phys. Rev. D **58**, 105009 (1998).
[9] A. Hashimoto and Y. Oz, Aspects of QCD dynamics from string theory, Nucl. Phys. **B548**, 167 (1999).
[10] C. Csaki, Y. Oz, J. Russo, and J. Terning, Large N QCD from rotating branes, Phys. Rev. D **59**, 065012 (1999).
[11] J. A. Minahan, Glueball mass spectra and other issues for supergravity duals of QCD models, J. High Energy Phys. 01 (1999) 020.
[12] R. C. Brower, S. D. Mathur, and C. I. Tan, Glueball spectrum for QCD from AdS supergravity duality, Nucl. Phys. **B587**, 249 (2000).
[13] E. Caceres and R. Hernandez, Glueball masses for the deformed conifold theory, Phys. Lett. B **504**, 64 (2001).
[14] H. Boschi-Filho and N. R. F. Braga, Gauge/string duality and scalar glueball mass ratios, J. High Energy Phys. 05 (2003) 009.
[15] H. Boschi-Filho and N. R. F. Braga, QCD/string holographic mapping and glueball mass spectrum, Eur. Phys. J. C **32**, 529 (2004).
[16] R. Apreda, D. E. Crooks, N. J. Evans, and M. Petrini, Confinement, glueballs and strings from deformed AdS, J. High Energy Phys. 05 (2004) 065.
[17] X. Amador and E. Caceres, Spin two glueball mass and glueball regge trajectory from supergravity, J. High Energy Phys. 11 (2004) 022.
[18] N. Evans, J. P. Shock, and T. Waterson, Towards a perfect QCD gravity dual, Phys. Lett. B **622**, 165 (2005).
[19] E. Caceres and C. Nunez, Glueballs of super Yang-Mills from wrapped branes, J. High Energy Phys. 09 (2005) 027.
[20] H. Boschi-Filho, N. R. F. Braga, and H. L. Carrion, Glueball Regge trajectories from gauge/string duality and the Pomeron, Phys. Rev. D **73**, 047901 (2006).
[21] P. Colangelo, F. De Fazio, F. Jugeau, and S. Nicotri, On the light glueball spectrum in a holographic description of QCD, Phys. Lett. B **652**, 73 (2007).
[22] E. Folco Capossoli and H. Boschi-Filho, Odd spin glueball masses and the Odderon Regge trajectories from the holographic hardwall model, Phys. Rev. D **88**, 026010 (2013).

[23] E. Folco Capossoli and H. Boschi-Filho, Glueball spectra and Regge trajectories from a modified holographic softwall model, Phys. Lett. B **753**, 419 (2016).
[24] E. Folco Capossoli, D. Li, and H. Boschi-Filho, Dynamical corrections to the anomalous holographic soft-wall model: The Pomeron and the Odderon, Eur. Phys. J. C **76**, 320 (2016).
[25] E. F. Capossoli, J. P. M. Graça, and H. Boschi-Filho, AdS/QCD oddball masses and the Odderon Regge trajectory from a twist-five operator approach, Phys. Rev. D **105**, 026026 (2022).
[26] T. Sakai and S. Sugimoto, Low energy hadron physics in holographic QCD, Prog. Theor. Phys. **113**, 843 (2005).
[27] T. Sakai and S. Sugimoto, More on a holographic dual of QCD, Prog. Theor. Phys. **114**, 1083 (2005).
[28] G. F. de Teramond and S. J. Brodsky, Hadronic spectrum of a holographic dual of QCD, Phys. Rev. Lett. **94**, 201601 (2005).
[29] J. Erlich, E. Katz, D. T. Son, and M. A. Stephanov, QCD and a holographic model of hadrons, Phys. Rev. Lett. **95**, 261602 (2005).
[30] L. Da Rold and A. Pomarol, Chiral symmetry breaking from five dimensional spaces, Nucl. Phys. **B721**, 79 (2005).
[31] K. Ghoroku, N. Maru, M. Tachibana, and M. Yahiro, Holographic model for hadrons in deformed AdS_5 background, Phys. Lett. B **633**, 602 (2006).
[32] A. Karch, E. Katz, D. T. Son, and M. A. Stephanov, Linear confinement and AdS/QCD, Phys. Rev. D **74**, 015005 (2006).
[33] S. J. Brodsky and G. F. de Teramond, Hadronic spectra and light-front wavefunctions in holographic QCD, Phys. Rev. Lett. **96**, 201601 (2006).
[34] H. Hata, T. Sakai, S. Sugimoto, and S. Yamato, Baryons from instantons in holographic QCD, Prog. Theor. Phys. **117**, 1157 (2007).
[35] H. Forkel, M. Beyer, and T. Frederico, Linear square-mass trajectories of radially and orbitally excited hadrons in holographic QCD, J. High Energy Phys. 07 (2007) 077.
[36] U. Gursoy and E. Kiritsis, Exploring improved holographic theories for QCD: Part I, J. High Energy Phys. 02 (2008) 032.
[37] U. Gursoy, E. Kiritsis, and F. Nitti, Exploring improved holographic theories for QCD: Part II, J. High Energy Phys. 02 (2008) 019.
[38] J. Erdmenger, N. Evans, I. Kirsch, and E. Threlfall, Mesons in Gauge/gravity duals—A review, Eur. Phys. J. A **35**, 81 (2008).
[39] A. Vega and I. Schmidt, Scalar hadrons in $AdS_5 x S^5$, Phys. Rev. D **78**, 017703 (2008).
[40] W. de Paula, T. Frederico, H. Forkel, and M. Beyer, Dynamical AdS/QCD with area-law confinement and linear Regge trajectories, Phys. Rev. D **79**, 075019 (2009).
[41] P. Colangelo, F. De Fazio, F. Giannuzzi, F. Jugeau, and S. Nicotri, Light scalar mesons in the soft-wall model of AdS/QCD, Phys. Rev. D **78**, 055009 (2008).
[42] Z. Abidin and C. E. Carlson, Nucleon electromagnetic and gravitational form factors from holography, Phys. Rev. D **79**, 115003 (2009).
[43] T. Gutsche, V. E. Lyubovitskij, I. Schmidt, and A. Vega, Dilaton in a soft-wall holographic approach to mesons and baryons, Phys. Rev. D **85**, 076003 (2012).
[44] D. Li, M. Huang, and Q. S. Yan, A dynamical soft-wall holographic QCD model for chiral symmetry breaking and linear confinement, Eur. Phys. J. C **73**, 2615 (2013).
[45] S. J. Brodsky, G. F. de Teramond, H. G. Dosch, and J. Erlich, Light-front holographic QCD and emerging confinement, Phys. Rep. **584**, 1 (2015).
[46] J. Sonnenschein, Holography inspired stringy hadrons, Prog. Part. Nucl. Phys. **92**, 1 (2017).
[47] E. Folco Capossoli, M. A. Martín Contreras, D. Li, A. Vega, and H. Boschi-Filho, Hadronic spectra from deformed AdS backgrounds, Chin. Phys. C **44**, 064104 (2020).
[48] S. S. Afonin, Towards reconciling the holographic and lattice descriptions of radially excited hadrons, Eur. Phys. J. C **80**, 723 (2020).
[49] M. Rinaldi and V. Vento, Meson and glueball spectroscopy within the graviton soft wall model, Phys. Rev. D **104**, 034016 (2021).
[50] H. R. Grigoryan and A. V. Radyushkin, Form factors and wave functions of vector mesons in holographic QCD, Phys. Lett. B **650**, 421 (2007).
[51] K. A. Mamo and I. Zahed, Neutrino-nucleon DIS from holographic QCD: PDFs of sea and valence quarks, form factors, and structure functions of the proton, Phys. Rev. D **104**, 066010 (2021).
[52] P. V. Landshoff, Pomerons, in *Talk at Meeting on Elastic Scattering and Diffraction*, edited by V. Kundrat and P. Zavada (2002); arXiv:hep-ph/0108156.
[53] V. S. Fadin and L. N. Lipatov, BFKL pomeron in the next-to-leading approximation, Phys. Lett. B **429**, 127 (1998).
[54] H. B. Meyer and M. J. Teper, Glueball Regge trajectories and the pomeron: A lattice study, Phys. Lett. B **605**, 344 (2005).
[55] C. J. Morningstar and M. J. Peardon, The glueball spectrum from an anisotropic lattice study, Phys. Rev. D **60**, 034509 (1999).
[56] Y. Chen, A. Alexandru, S. J. Dong, T. Draper, I. Horvath, F. X. Lee, K. F. Liu, N. Mathur, C. Morningstar, M. Peardon *et al.*, Glueball spectrum and matrix elements on anisotropic lattices, Phys. Rev. D **73**, 014516 (2006).
[57] B. Lucini and M. Teper, $SU(N)$ gauge theories in four-dimensions: Exploring the approach to $N = \infty$, J. High Energy Phys. 06 (2001) 050.
[58] E. Gregory, A. Irving, B. Lucini, C. McNeile, A. Rago, C. Richards, and E. Rinaldi, Towards the glueball spectrum from unquenched lattice QCD, J. High Energy Phys. 10 (2012) 170.
[59] W. Sun, L. C. Gui, Y. Chen, M. Gong, C. Liu, Y. B. Liu, Z. Liu, J. P. Ma, and J. B. Zhang, Glueball spectrum from $N_f = 2$ lattice QCD study on anisotropic lattices, Chin. Phys. C **42**, 093103 (2018).
[60] A. Athenodorou and M. Teper, The glueball spectrum of SU(3) gauge theory in $3 + 1$ dimensions, J. High Energy Phys. 11 (2020) 172.

[61] G. 't Hooft, A planar diagram theory for strong interactions, Nucl. Phys. **B72**, 461 (1974).
[62] P. Breitenlohner and D. Z. Freedman, Stability in gauged extended supergravity, Ann. Phys. (N.Y.) **144**, 249 (1982).
[63] P. Lebiedowicz, O. Nachtmann, and A. Szczurek, Central exclusive diffractive production of a single photon in high-energy proton-proton collisions within the tensor-Pomeron approach, Phys. Rev. D **107**, 074014 (2023).